Mechanism for the Formaldehyde to Formic Acid and the Formic Acid to Carbon Dioxide Conversions Mediated by an Iron-Oxo Species

Takashi Yumura,[†,‡] Tatsuhiko Amenomori,[‡] Yoshihisa Kagawa,[‡] and Kazunari Yoshizawa*[,†]

Institute for Fundamental Research of Organic Chemistry, Kyushu University, Fukuoka 812-8581, Japan, and Department of Molecular Engineering, Kyoto University, Kyoto 606-8501, Japan

Received: June 12, 2001; In Final Form: November 13, 2001

The mechanism and energetics for the formaldehyde to formic acid and the formic acid to carbon dioxide conversions are investigated using the FeO^+ complex as an oxidant from theoretical calculations at the B3LYP DFT level. In the oxidation processes, there are a lot of reaction branches which are comparable in energy. The elementary processes can be viewed as C−H and O−H cleavage reactions by oxo and hydroxo ligands as well as OH group migrations. In formaldehyde oxidation, the initially formed complex OFe^+-OCH_2 is converted by a C−H bond cleavage to intermediate $HO-Fe^+-OCH$, which is next transformed to the formic acid complex $Fe^+-OCHOH$ by an OH ligand migration and to the carbon monoxide complex H_2O-Fe^+-CO by a C−H bond cleavage. There are two possible reaction pathways for the formic acid to carbon dioxide conversion, both reaction pathways being downhill and highly exothermic. In an energetically favorable reaction pathway, complex $OFe^+-OCHOH$ is first converted to intermediate $HO-Fe^+-OCHO$ by an O−H bond cleavage, and after that, $HO-Fe^+-OCHO$ is transformed to the product complex $H_2O-Fe^+-O_2C$ by a C−H bond cleavage. Formaldehyde and formic acid are easily oxidized by an excess of oxidants to carbon dioxide and carbon monoxide. The overall reaction from methane to carbon dioxide is exothermic by 117.9 kcal/mol, and there is no high barrier after methanol formation, which can cause the well-known overoxidation problem in methane and alkane oxidation. Our calculations are in good agreement with previous experiments on methane oxidation over Fe−ZSM-5 zeolite with respect to the product branching ratio, suggesting that a surface iron-oxo species should have relevance to the interesting catalytic functions of Fe−ZSM-5 zeolite.

Introduction

Selective oxidation of methane to methanol under mild conditions has been an attractive issue in modern industrial chemistry.[1−10] Methanol produced from the oxidation of methane is not stable in the presence of an excess of oxidants and is further oxidized to formaldehyde, formic acid, and carbon dioxide, which is known as an overoxidation problem. It is difficult to control the oxidation reactions of methane to methanol and formaldehyde without forming further oxidized products. For example, Anderson and Tsai[11] and Panov et al.[12] reported that methane is converted mainly to carbon monoxide and carbon dioxide using N_2O as an oxidant over Fe−ZSM-5 zeolite at high temperature. On the other hand, Raja and Ratnasamy[13] reported that the oxidation of methane to methanol and formaldehyde can be selectively performed using phthalocyanine complexes of Fe and Cu on the zeolite frameworks as catalysts. According to their proposal, the overoxidation problem, especially the formation of carbon dioxide, arises from high catalysts concentrations and prolonged contact times. Although the selective oxidation reactions of alkanes to corresponding alcohols and aldehydes were extensively investigated,[14] our knowledge on the mechanism of the overoxidation reactions of methane is still lacking. We can illuminate these black box reactions by means of computational quantum chemistry. In previous papers,[15,16] we considered with density functional theory (DFT) the catalytic functions of "α-oxygen", a surface oxygen species responsible for the direct hydroxylation of methane over Fe−ZSM-5 zeolite,[12] and we demonstrated using a reasonable model involving an iron-oxo species on the AlO_4 surface site that the mechanism of "α-oxygen"-catalyzed methane hydroxylation is essentially identical to that of methane hydroxylation by FeO^+.[17,18] The bare FeO^+ complex is helpful in understanding various oxidation reactions catalyzed by transition-metal oxides because in the gas-phase FeO^+ mediates a variety of oxidation reactions, which give us a useful hint about elementary steps in catalytic oxidation processes.

Schwarz, Schröder, and co-workers have studied in detail the methane to methanol conversion by FeO^+,[18] which is formed from the reaction of Fe^+ with pulsed-in N_2O[19] under Fourier transform ion cyclotron resonance (FTICR) conditions. A key step in the conversion of methane to methanol is the C−H bond activation because of its significant bond dissociation energy (104 kcal/mol). They proposed that complex $HO-Fe^+-CH_3$ is involved in the reaction as an intermediate. Moreover, they investigated the methanol-formaldehyde conversion by FeO^+ under FTICR conditions and predicted that complex $HO-Fe^+-OCH_3$ should play a role as a central intermediate in the oxidation reaction.[20] From DFT calculations, we have investigated the mechanism and energetics of the methane−methanol[21] and the methanol−formaldehyde[22] conversions by FeO^+. The conversion of methane to methanol occurs in a two-step manner, as shown in Figure 1; it proceeds at the iron active center through concerted hydrogen and methyl migrations.[21] In the

* To whom correspondence should be addressed. E-mail: kazunari@ms.ifoc.kyushu-u.ac.jp

† Institute for Fundamental Research of Organic Chemistry, Kyushu University.

‡ Department of Molecular Engineering, Kyoto University.

10.1021/jp0122225 CCC: $22.00
Published on Web 01/04/2002

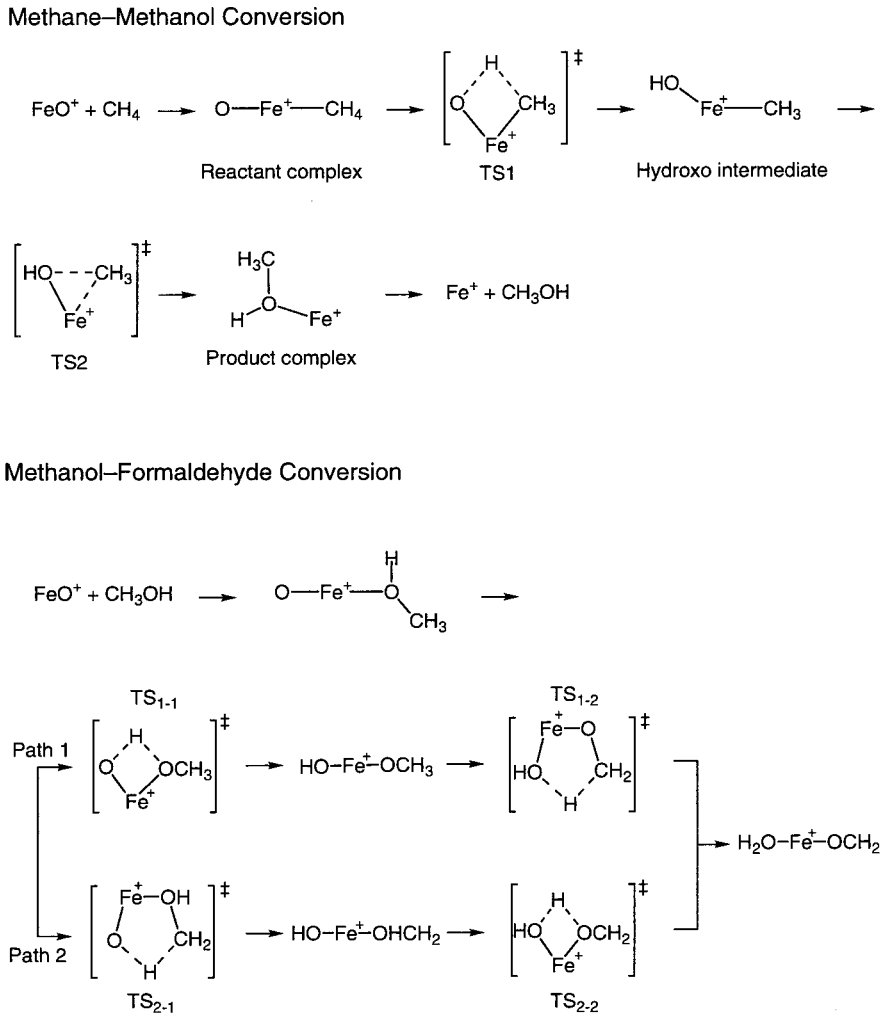

Figure 1. Reaction pathways for the direct methane-methanol and the methanol-formaldehyde conversions mediated by FeO^+.

SCHEME 1

$$CH_4 \xrightarrow[FeO^+]{} CH_3OH \xrightarrow[FeO^+]{} CH_2O \xrightarrow[FeO^+]{\text{Path A}} HCOOH \xrightarrow[FeO^+]{\text{Path B}} CO_2$$

methanol−formaldehyde conversion, there are two competitive reaction pathways.[22] In Path 1, the H atom of the OH group of methanol is first abstracted by the oxo group of FeO^+ via TS_{1-1} leading to the intermediate complex $HO-Fe^+-OCH_3$, and after that one of the H atoms of the OCH_3 group is shifted to the OH ligand via TS_{1-2} to form the product complex $H_2O-Fe^+-OCH_2$. In Path 2, one of the H atoms of the CH_3 group of methanol is abstracted by the oxo group via TS_{2-1} leading to intermediate $HO-Fe^+-OHCH_2$, and then, the H atom of the $OHCH_2$ group is shifted to the OH ligand via TS_{2-2} to give the product complex $H_2O-Fe^+-OCH_2$.

The computed energetics for the oxidation of methanol to formaldehyde suggests that in general produced alcohols undergo further oxidation toward aldehydes, carboxylic acids, and carbon dioxide in the presence of an excess of oxidants. In this article, we describe the mechanism for the oxidation reactions of formaldehyde to formic acid (Path A) and of formic acid to carbon dioxide (Path B); see Scheme 1. From DFT calculations of the methane oxidation processes by FeO^+, we shed light on the overoxidation problem in the catalytic oxidation of methane and other alkanes.

Method of Calculation. We carried out quantum chemical calculations on the basis of the hybrid Hartree−Fock/density functional theory (B3LYP) method[23,24] using the Gaussian 98 ab initio program package.[25] The B3LYP method consists of the Slater exchange, the Hartree−Fock exchange, the exchange functional of Becke,[23] the correlation functional of Lee, Yang, and Parr (LYP),[24] and the correlation functional of Vosko, Wilk, and Nusair (VWN).[26] We optimized local energy minima corresponding to reactants, products, and intermediates and saddle points corresponding to transition states. Harmonic vibrational frequencies were systematically computed to confirm that each optimized geometry corresponds to a local minimum that has only real frequencies or a saddle point that has only one imaginary frequency. For the Fe atom we used the (14s9p5d) primitive set of Wachters[27] supplemented with one polarization f-function ($\alpha = 1.05$), resulting in a (611111111|51111|311|1) [9s5p3d1f] contraction,[28] and for the H, C, and O atoms we used the 6-311G** basis set.[29] The spin-unrestricted method was applied to the open-shell systems. It was confirmed from computed $<S^2>$ values that spin contamination included in the calculations is within 0.54% after annihilation of higher spin states. We computed the bond dissociation energy of the $^6\Sigma^+$ state of FeO^+ to look at the applicability of this DFT method. This quantity was computed to be 75.2 kcal/mol, which is in good agreement with an experimental value of 81.4 ± 1.4 kcal/mol.[30]

Results and Discussion

Formaldehyde Oxidation by FeO^+. Formaldehyde oxidation mediated by FeO^+ is expected to occur as in Scheme 2, in which

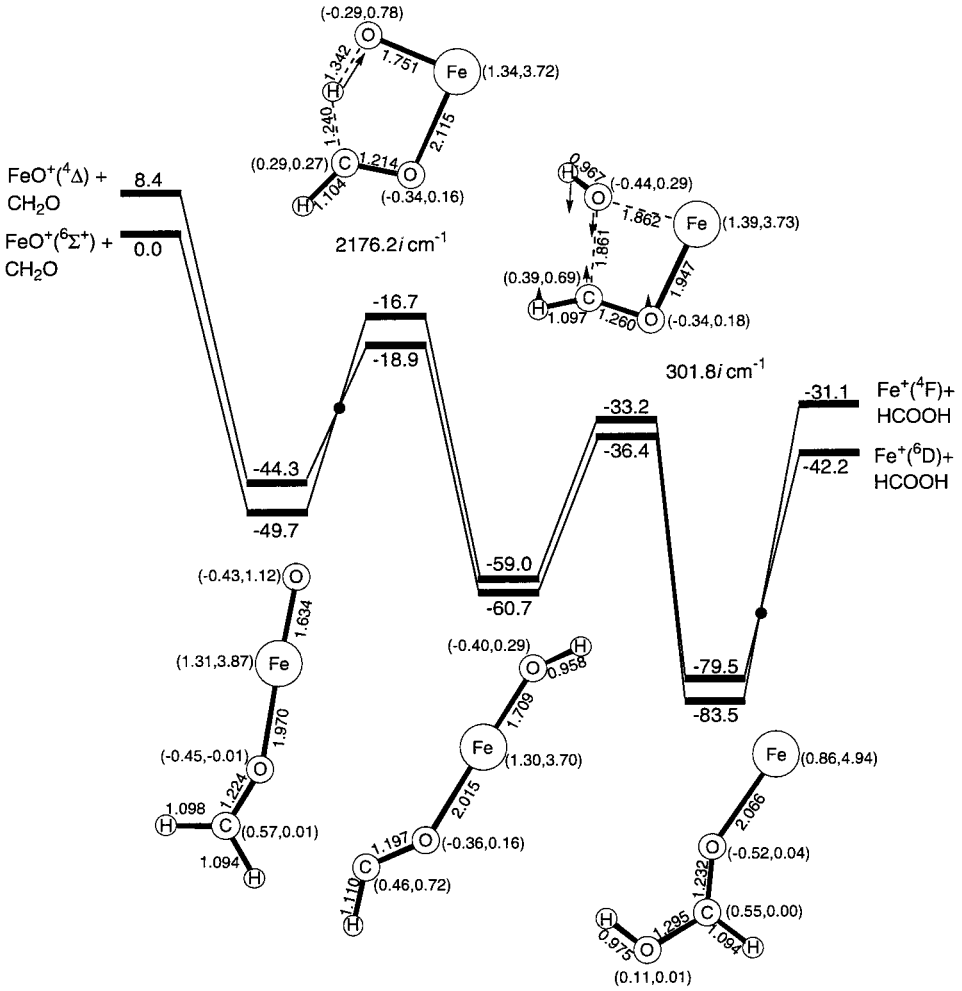

Figure 2. Potential energy diagrams for the conversion of formaldehyde to formic acid by FeO^+ in the sextet and the quartet reaction pathways at the B3LYP/6-311G** level including zero-point energy corrections. Relative energies are in units of in kcal/mol. Optimized structures, charges, and spin densities (charge, spin density) of intermediates and transition states in the sextet reaction pathway are shown. Bond lengths are in Å.

SCHEME 2

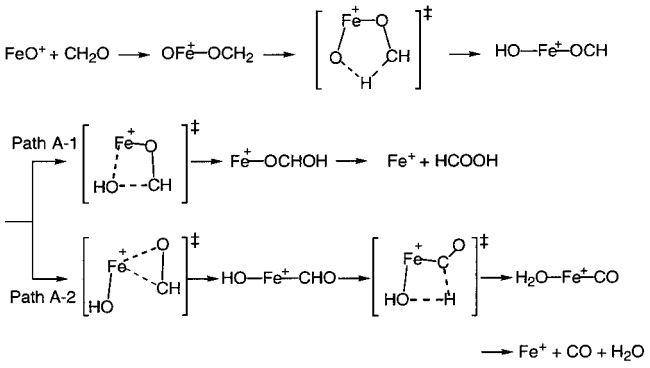

we assume that complex OFe^+-OCH_2 should be formed in the initial stages of the reaction. DFT calculations predict a scenario on the chemical processes as follows. The reactant complex is converted to intermediate $HO-Fe^+-OCH$ via the five-centered transition state for the H atom abstraction. After the formation of $HO-Fe^+-OCH$, there are two possible reaction pathways, as indicated in Scheme 2. Path A-1 is a branch that leads to formic acid and Path A-2 is another branch that finally leads to carbon monoxide. In Path A-1, the OH ligand of $HO-Fe^+-OCH$ is migrated toward the carbon atom of the OCH group via the four-centered transition state, resulting in $Fe^+-OCHOH$. In the first half of Path A-2, $HO-Fe^+-OCH$ is transformed into $HO-Fe^+-CHO$ via the three-centered transition state, and in the second half, $HO-Fe^+-CHO$ is converted to H_2O-Fe^+-CO via the four-centered transition state and finally water and carbon monoxide are released from the final complex.

Formaldehyde to Formic Acid Conversion (Path A-1). Let us first look at the reaction mechanism and energetics for the formaldehyde to formic acid conversion along Path A-1. Figure 2 shows computed energy diagrams for Path A-1 in the sextet and the quartet reaction pathways and optimized geometries of the reaction intermediates and the transition states in the sextet state. A closed circle stands for a crossing point of the energy diagrams. The general profile of Figure 2 is consistent with the two-state reactivity paradigm proposed by Shaik et al.[31] because the two potential energy surfaces are close-lying and in fact there are crossing points in the entrance and the exit channels. Thus, both sextet and quartet potential energy surfaces have relevance to the course of this reaction. In the initial stages of the reaction, FeO^+ and formaldehyde come into contact to form the reactant complex OFe^+-OCH_2 with a binding energy of 49.7 and 52.7 kcal/mol in the sextet and the quartet states, respectively. Because the HOMO of formaldehyde has a larger orbital coefficient on the oxygen atom, it is reasonable to form an Fe−O bond rather than an Fe−C bond. The total atomic (Mulliken) charge of formaldehyde is +0.12, the atomic charge of the carbon atom changes from +0.25 in formaldehyde to +0.57 in the reactant complex, and that of the oxygen atom changes from −0.25 to −0.45. This computational result is due to the polar character of the carbonyl group, as indicated by

SCHEME 3

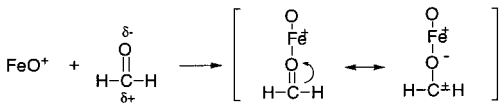

SCHEME 4

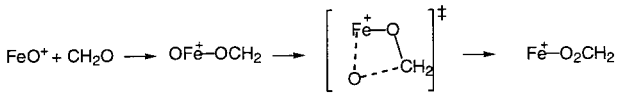

the resonance structures in Scheme 3. In the reactant complex OFe^+-OCH_2, the carbonyl carbon atom bears substantial positive charge through the electron transfer to the carbonyl oxygen atom to lead to the second resonance structure. The polar character of the carbonyl group plays an important role in the oxidation of formaldehyde. The increasing polarizability can be explained from a second-order perturbational treatment, as indicated in Appendix.

After the formation of OFe^+-OCH_2, an H atom of formaldehyde is abstracted by the oxo group of FeO^+ via the five-centered transition state. This H atom abstraction gives rise to the radical intermediate $HO-Fe^+-OCH^\bullet$, in which the carbon atom has a large spin density of +0.72 in the sextet state. In this chemical process, the C−H bond is cleaved in a homolytic manner, and the H atom is migrated to the oxygen atom of FeO^+ to form a new O−H bond. Although the activation energies for this process are 33.0 and 25.4 kcal/mol relative to OFe^+-OCH_2 in the sextet and the quartet reaction pathways, respectively, this reacting system can pass over the potential energy barrier because this transition state lies well below the dissociation limit toward formaldehyde and FeO^+. After the formation of $HO-Fe^+-OCH^\bullet$, the recombination of the OH and the CHO groups occurs on the complex, resulting in $Fe^+-OCHOH$. A calculated activation energy for this process in the sextet reaction pathway is 25.8 kcal/mol and that in the quartet reaction pathway is 24.3 kcal/mol relative to $HO-Fe^+-OCH^\bullet$, but this energy barrier is also accessible from the viewpoint of energetics. The formic acid complex $Fe^+-OCHOH$ is energetically the most stable in the reaction pathway, and it lies 79.5 and 83.5 kcal/mol below the dissociation limit in the sextet and the quartet reaction pathways, respectively. Finally, $Fe^+-OCHOH$ releases Fe^+ and formic acid using the internal energy acquired. The overall conversion of formaldehyde to formic acid is exothermic and the transition states involved are low-lying, and therefore, the reaction should easily take place.

The reactant complex can be converted to a complex involving dioxymethylene as a byproduct, as indicated in Scheme 4. In this process the O atom of FeO^+ is migrated to the C atom of formaldehyde via a four-centered transition state, leading to the dioxymethylene complex. The activation energy was computed to be −27.1 and −25.8 kcal/mol relative to the dissociation limit to FeO^+ and formaldehyde in the sextet and quartet states, respectively; hence, the conversion of formaldehyde to dioxymethylene is likely to take place. In fact, dioxymethylene is detected by FT-IR measurements in oxidation reactions of formaldehyde on metal oxides.[32]

Formaldehyde to Carbon Monoxide Conversion (Path A-2). Let us next look at the energetics for the formaldehyde to carbon monoxide conversion by FeO^+ along Path A-2. Figure 3 shows computed energy diagrams for Path A-2 in the sextet and the quartet reaction pathways. Optimized geometries of the reaction intermediates and the transition states in the sextet state are also presented. This reaction is also exothermic. The first half of Path A-2 is identical to that of Path A-1. After $HO-Fe^+-OCH^\bullet$ is formed, it is converted to $HO-Fe^+-CHO$ via the three-centered transition state. The carbon atom of $HO-Fe^+-OCH^\bullet$ is migrated toward Fe^+ with an activation energy of 6.8 and 2.2 kcal/mol in the sextet and the quartet reaction pathways, respectively. The spin density on the carbon atom of $HO-Fe^+-CHO$ is +0.17 in the sextet state, this value being small in comparison with that of $HO-Fe^+-OCH^\bullet$. Once the Fe−C bond is formed, the C−H bond of the CHO group is activated through the electron transfer from the CHO group to the FeOH group. Because the computed activation energy for the H atom abstraction from the CHO group in the sextet pathway is −35.9 kcal/mol and that in the quartet pathway is −47.6 kcal/mol relative to the dissociation limit, this reaction should easily take place. The product complex H_2O-Fe^+-CO is formed as a result of the H atom abstraction from the CHO group, and it is energetically the most stable intermediate in Path A-2. Carbon monoxide is one of the main products in methane oxidation by N_2O over Fe−ZSM-5 zeolite at high temperature;[11,12] therefore, the mechanistic aspect of Path A-2 can give a hint with respect to the mechanism and energetics of the overoxidation problem.

Let us compare the energetics for the oxidation reactions of formaldehyde via Paths A-1 and A-2. Both A-1 and A-2 are exothermic, and formaldehyde should be spontaneously converted into formic acid and carbon monoxide in the presence of FeO^+. A difference between Paths A-1 and A-2 is the spin density on the carbon atom of the intermediates $HO-Fe^+-OCH^\bullet$ and $HO-Fe^+-CHO$. Although the mechanisms of Paths A-1 and A-2 are quite different, they are comparable in energy. According to DFT calculations, the carbon monoxide complex in Path A-2 is 32.2 kcal/mol more stable than the formic acid complex in Path A-1 in the quartet reaction pathway, which suggests that formic acid can be released more easily than carbon monoxide, and formic acid should be further oxidized.

Formic Acid Oxidation by FeO^+. To increase our understanding of the overoxidation problem, we must consider the further oxidation of formic acid. First we assume that the two reactant complexes, $OFe^+-OCHOH$ and $OFe^+-OHCHO$, are formed in the initial stages of the reaction. In $OFe^+-OCHOH$ the carbonyl oxygen atom coordinates to the Fe^+ ion as a ligand, whereas in $OFe^+-OHCHO$ the hydroxyl oxygen atom coordinates. DFT calculations tell us that $OFe^+-OCHOH$ is 17.9 and 18.9 kcal/mol more stable than $OFe^+-OHCHO$ in the sextet and the quartet states, respectively. Therefore, it is reasonable to restrict our discussion to the formic acid oxidation reactions that start from $OFe^+-OCHOH$. There are two possible reaction pathways for the conversion of formic acid to carbon dioxide, as shown in Scheme 5. In Path B-1, the reactant complex is converted to $HO-Fe^+-OCOH$ via the five-centered transition state for the C−H bond cleavage by the oxo group of FeO^+. After the formation of $HO-Fe^+-OCOH$, the O−H bond of the OCOH group is activated by the OH ligand to result in $H_2O-Fe^+-O_2C$. On the other hand, Path B-2 involves the O−H bond activation by the oxo group via the six-centered transition state in the initial stages and as a result $HO-Fe^+-OCHO$ is formed. After that, the C−H bond cleavage by the OH ligand gives rise to $H_2O-Fe^+-O_2C$.

Path B-1. Figure 4 shows computed energy diagrams for Path B-1 in the sextet and the quartet reaction pathways and optimized geometries of the reaction species in the sextet state. In the initial stages of the reaction, FeO^+ and formic acid come into contact with a binding energy of 59.1 and 62.3 kcal/mol in the sextet and the quartet pathways, respectively. Interestingly,

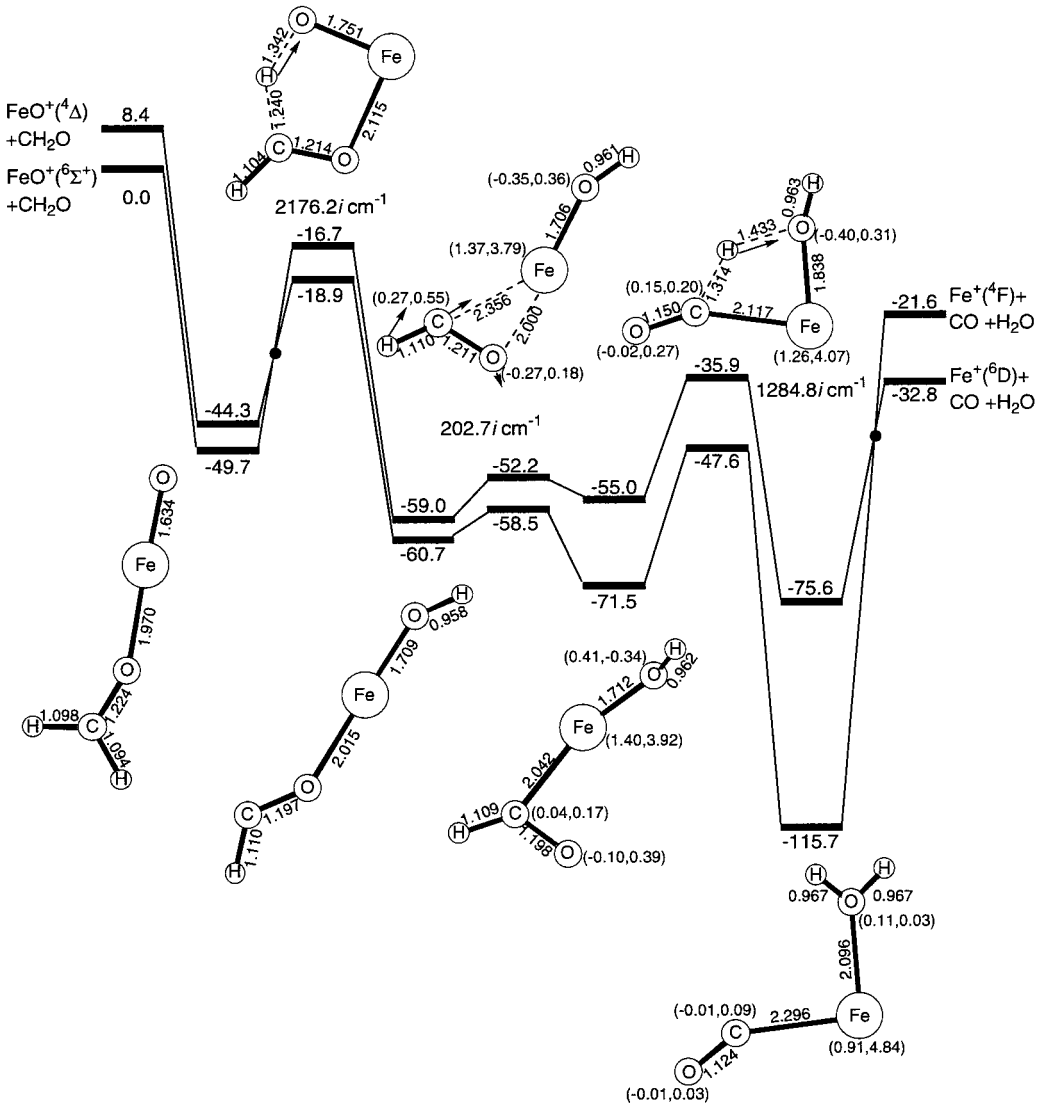

Figure 3. Potential energy diagrams for the conversion of formaldehyde to carbon monoxide by FeO^+ in the sextet and the quartet reaction pathways at the B3LYP/6-311G** level including zero-point energy corrections. Relative energies are in units of in kcal/mol. Optimized structures, charges, and spin densities (charge, spin density) of intermediates and transition states in the sextet reaction pathway are shown. Bond lengths are in Å.

SCHEME 5

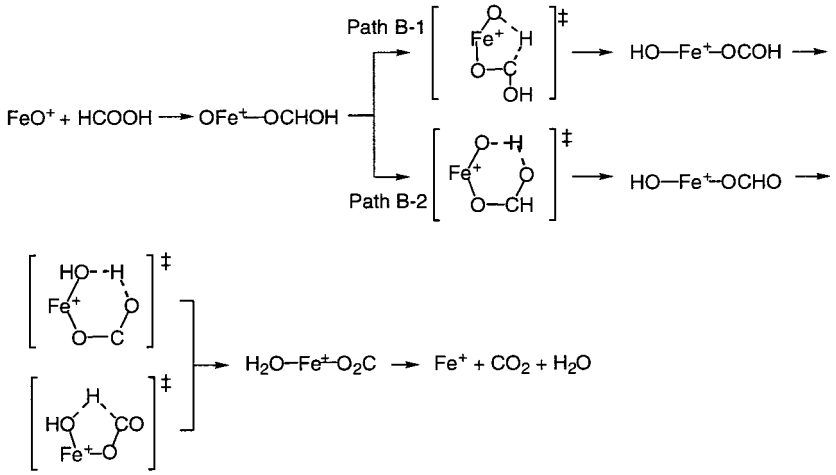

the C−OH bond in the reactant complex is slightly shortened and the C═O bond is slightly elongated in comparison with those of free formic acid. This geometrical change can be explained by the resonance forms indicated in Scheme 6. The last resonance that can contribute to the short C−OH bond and the long C═O bond is significantly stabilized in the presence of FeO^+. The geometrical features of the reactant complex can be explained from these resonance forms.

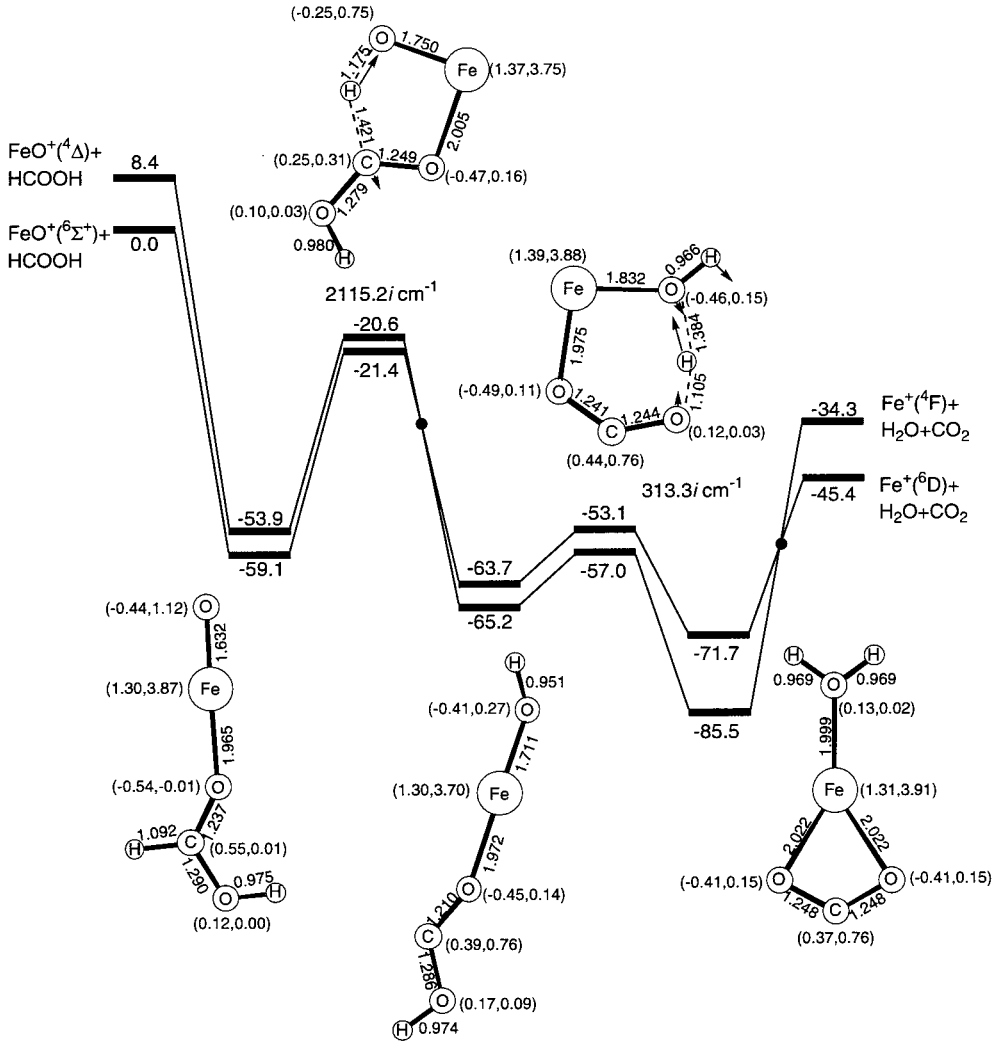

Figure 4. Potential energy diagrams for the conversion of formic acid to carbon dioxide by FeO^+ via Path B-1 in the sextet and the quartet reaction pathways at the B3LYP/6-311G** level including zero-point energy corrections. Relative energies are in units of in kcal/mol. Optimized structures, charges, and spin densities (charge, spin density) of intermediates and transition states in the sextet reaction pathway are shown. Bond lengths are in Å.

SCHEME 6

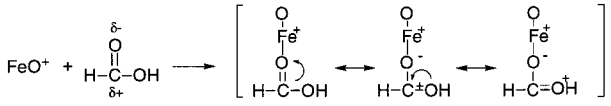

After the formation of $OFe^+-OCHOH$, the C−H bond is dissociated by the oxo group of FeO^+ and the radical intermediate $HO-Fe^+-OCOH^\bullet$ is formed as a result. The C−H bond dissociation can take place in a homolytic manner because the carbon atom in $HO-Fe^+-OCOH^\bullet$ has a spin density of +0.76 in the sextet state. The activation energy for the H atom abstraction in the sextet reaction pathway was computed to be 37.7 kcal/mol and that in the quartet reaction pathway was 33.3 kcal/mol measured from the reactant complex. The reacting system can pass over this transition state using the high internal energy. In the next process, intermediate $HO-Fe^+-OCOH^\bullet$ is converted to the product complex $H_2O-Fe^+-O_2C$. In this electronic process, the O−H bond of the CO_2H group is dissociated by the hydroxo ligand with an activation energy of 10.6 and 8.2 kcal/mol relative to $HO-Fe^+-OCOH^\bullet$ in the sextet and the quartet reaction pathways, respectively. The product complex $H_2O-Fe^+-O_2C$, the most stable species in Path B-1, releases water and carbon dioxide in the final step.

SCHEME 7

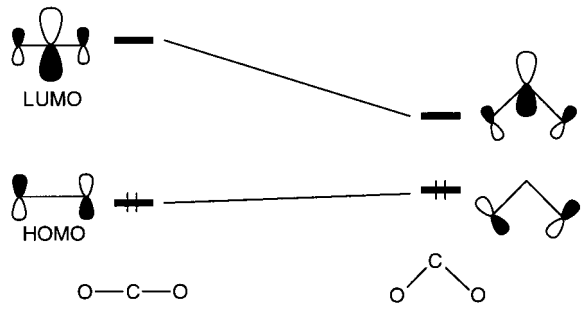

It is noting that the carbon dioxide in the product complex is bent. This can be explained by a qualitative Walsh diagram indicated in Scheme 7. The HOMO of linear carbon dioxide is a nonbonding orbital and the LUMO is a pπ^* orbital that has a larger orbital coefficient on the central carbon atom. This diagram tells us that the LUMO is significantly pushed down upon bending, whereas the HOMO is slightly pushed up. Because the LUMO of carbon dioxide is partially filled in the carbon dioxide complex, the complex is stabilized in energy when the carbon dioxide is bent. In fact, the carbon dioxide in the product complex has a total charge of −0.45. Because the LUMO has a large orbital coefficient on the central carbon atom,

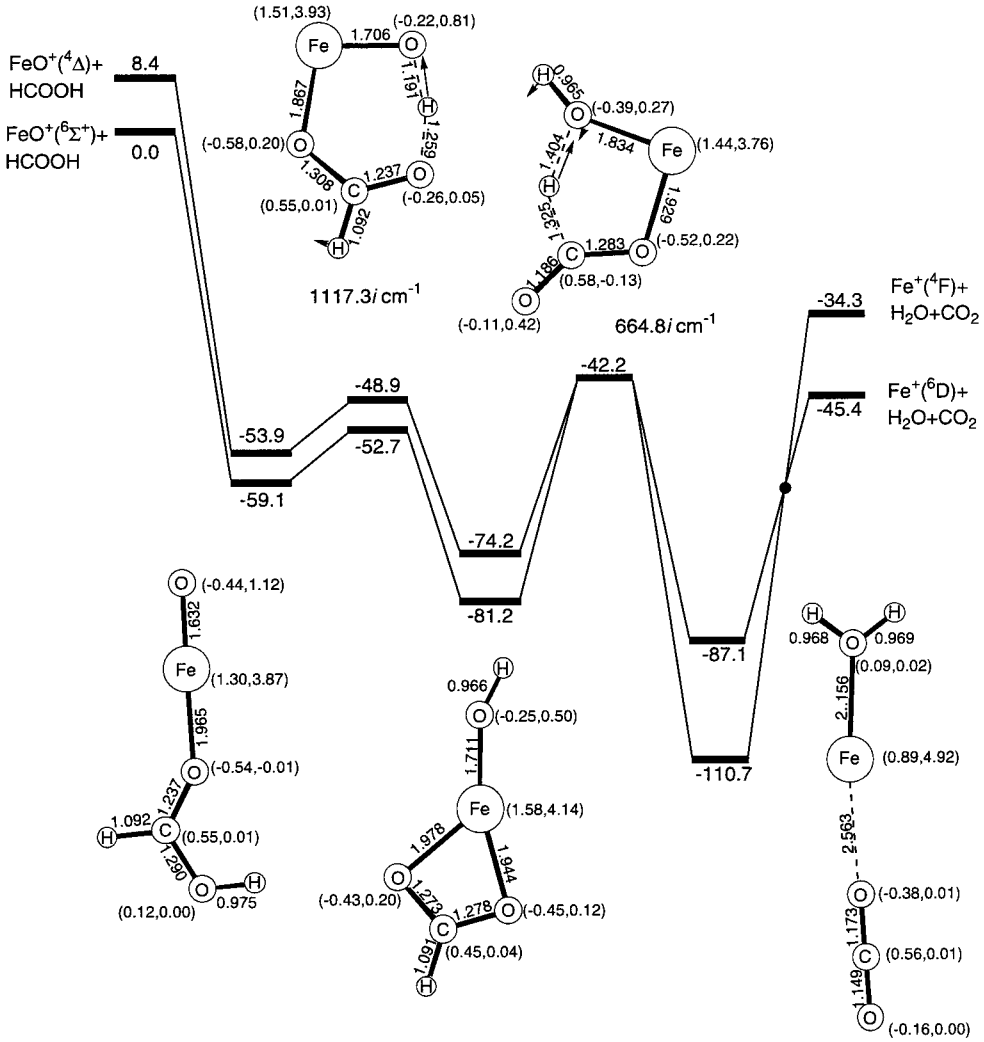

Figure 5. Potential energy diagrams for the conversion of formic acid to carbon dioxide by FeO^+ via Path B-2 in the sextet and the quartet reaction pathways at the B3LYP/6-311G** level including zero-point energy corrections. Relative energies are in units of in kcal/mol. Optimized structures, charges, and spin densities (charge, spin density) of intermediates and transition states in the sextet reaction pathway are shown. Bond lengths are in Å.

it is reasonable that the carbon atom has a significant spin density, which is a direct result from the homolytic C−H bond cleavage in Path B-1.

Path B-2. In contrast to Path B-1, in the initial stages of Path B-2 the O−H bond is cleaved by the oxo group of FeO^+, and after that the C−H bond is cleaved by the hydroxo ligand. Figure 5 shows computed energy diagrams for Path B-2 in the sextet and the quartet pathways. This reaction starts from the reactant complex OFe^+−OCHOH, as discussed above. The O−H bond dissociation requires an activation energy of 6.4 and 5.0 kcal/mol measured from the reactant complex in the sextet and the quartet pathways, respectively. The resultant intermediate HO−Fe^+−OCHO has an atomic charge of about −0.45 on each oxygen atom in the sextet state. This is reasonable in view of the following resonance structures in Scheme 8, in which the resonance structures of $OCHO^-$ and OCHO• and calculated atomic charges and spin densities are indicated in parentheses in this order. The calculated atomic charges on the oxygen atoms are −0.52 in $OCHO^-$, whereas those are −0.20 in OCHO•. The calculated atomic charges on the oxygen atoms in the intermediate are close to those of $OCHO^-$; hence, $OCHO^-$ is involved in HO−Fe^+−OCHO as a ligand, which suggests that the O−H bond is dissociated by the oxo group of FeO^+ in a heterolytic manner.

SCHEME 8

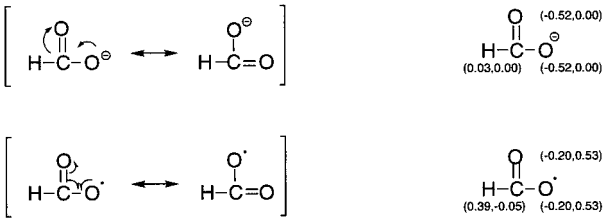

After the formation of HO−Fe^+−OCHO, the C−H bond is activated and cleaved by the hydroxo ligand, resulting in the final complex having water and carbon dioxide. The computed activation energy for the H atom migration in the sextet reaction pathway is 39.0 kcal/mol and that in the quartet reaction pathway is 32.0 kcal/mol relative to HO−Fe^+−OCHO.

Let us compare the energetics for the formic acid to carbon dioxide conversion reactions along Paths B-1 and B-2. The general energy profiles for Paths B-1 and B-2 are downhill toward the product direction. In the first stages of Path B-1, the C−H bond of formic acid is dissociated by the oxo group of FeO^+ in a homolytic manner, leading to intermediate HO−Fe^+−OCOH•, and after that the dissociation of the O−H bond by the hydroxo ligand results in the formation of carbon dioxide and water. In contrast, the O−H bond of formic acid is cleaved

CHART 1

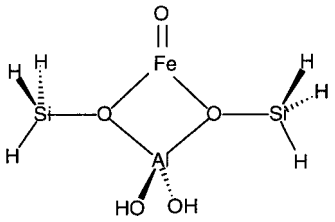

by the oxo group of FeO^+ in a heterolytic manner in the initial stages of Path B-2, and after that the final complex is formed via the five-centered transition state. In the reaction pathways for the conversion of formic acid, the C−H bond dissociation by the oxo group as well as by the hydroxo group is energetically the most difficult step. The C−H bond cleavage by the oxo group in Path B-1 follows the reactant complex OFe^+−OCHOH while that in Path B-2 follows intermediate HO−Fe^+−OCHO, as indicated in Scheme 5. The activation energy for the C−H bond cleavage in the sextet (quartet) reaction pathway along Path B-1 is −21.4 (−20.6) kcal/mol measured from the dissociation limit while that along Path B-2 is −42.2 (−42.2) kcal/mol. This is due to the difference in the stabilization of HO−Fe^+−OCHO and OFe^+−OCHOH. We conclude that Path B-2 is preferable in energy, but both reaction pathways are energetically favorable.

Methane Oxidation Mediated by FeO^+. Let us finally consider the energetics for the overall oxidation of methane to carbon dioxide. Previous experimental studies demonstrated that the final products in the oxidation of methane over Fe−ZSM-5 zeolite include carbon dioxide, carbon monoxide, and formaldehyde in high concentrations.[11,12] According to ref 11, carbon dioxide, carbon monoxide, and formaldehyde are produced in 87, 9.7, and 2.4% yields, respectively, in the oxidation of methane using N_2O at the reactant ratio CH_4 : N_2O = 60:40. The reactivity of the bare FeO^+ complex is of great use in aiding the understanding of various oxidation reactions mediated by transition-metal oxides. In our previous studies,[15,16] we set up a model of α-oxygen that is responsible for the direct oxidation of methane over Fe−ZSM-5 zeolite, as indicated in Chart 1. This model contains a coordinatively unsaturated iron-oxo species located on the AlO_4 anion site. If a coordinatively unsaturated iron species is generated on Fe−ZSM-5 zeolite, it should become an active center for the overoxidation process of methane.

Let us consider the energetics along the sextet pathway because the ground state of FeO^+ is a spin sextet. The conversion of methane to methanol is 12.6 kcal/mol exothermic.[21] However, the transition state for the H-atom abstraction from methane is comparable in energy with the dissociation limit, so the C−H bond dissociation is the rate-determining step in this important reaction. Once methane is converted to methanol, it is readily oxidized to formaldehyde by an excess of iron-oxo species[22] because there is no high-lying transition state in the course of reaction 2

$$FeO^+ + CH_4 \rightarrow CH_3OH + Fe^+ + 12.6\ \text{kcal/mol} \quad (1)$$

$$FeO^+ + CH_3OH \rightarrow CH_2O + H_2O + Fe^+ + 17.7\ \text{kcal/mol} \quad (2)$$

After the formation of formaldehyde, it is converted to formic acid and carbon monoxide. The formaldehyde to formic acid and the formaldehyde to carbon monoxide conversions are 42.2 and 32.8 kcal/mol exothermic, respectively. Thus, these reactions should take place more easily than the methane-methanol and the methanol-formaldehyde conversions. As shown in Figures 2 and 3, DFT calculations tell us that carbon monoxide is strongly bound to the iron active center while formic acid can be released and further oxidized in the presence of an excess of iron-oxo species. In fact, formic acid is not detected in the oxidation of methane over Fe−ZSM-5.[11,12] The oxidation reactions are energetically accelerated in the final stages; the conversion from formic acid to carbon dioxide is 45.4 kcal/mol exothermic. The overall reaction from methane to carbon dioxide is 117.9 kcal/mol exothermic, as indicated in reaction 6. Our calculations, which are in good agreement with the previous experiments[11,12] on methane oxidation over Fe−ZSM-5 zeolite with respect to the product branching ratio, suggest that a surface iron-oxo species should have relevance to the various catalytic functions of Fe−ZSM-5 zeolite

$$FeO^+ + CH_2O \rightarrow HCOOH + Fe^+ + 42.2\ \text{kcal/mol} \quad (3)$$

$$FeO^+ + CH_2O \rightarrow CO + H_2O + Fe^+ + 32.8\ \text{kcal/mol} \quad (4)$$

$$FeO^+ + HCOOH \rightarrow CO_2 + H_2O + Fe^+ + 45.4\ \text{kcal/mol} \quad (5)$$

$$4FeO^+ + CH_4 \rightarrow CO_2 + 2H_2O + 4Fe^+ + 117.9\ \text{kcal/mol} \quad (6)$$

Conclusions

We elucidated the mechanism of the formaldehyde to formic acid and the formic acid to carbon dioxide conversions from DFT computations at the B3LYP level of theory. We used the FeO^+ complex as an oxidant. One of our findings is that in the oxidation processes there are a lot of branches which are comparable in energy. We could classify the elementary processes into C−H and O−H cleavage reactions by oxo and hydroxo ligands as well as OH group migrations. In the reaction pathway for formaldehyde oxidation, an H atom of formaldehyde is first abstracted by the oxo group on the reactant complex OFe^+−OCH_2 and as a result intermediate HO−Fe^+−OCH is formed in the initial stages. This intermediate is next transformed to the formic acid complex Fe^+−OCHOH through an OH ligand migration and to the carbon monoxide complex H_2O−Fe^+−CO through an H atom migration. There are two possible reaction pathways for the formic acid to carbon dioxide conversion. In the first reaction pathway, complex OFe^+−OCHOH is converted to intermediate HO−Fe^+−OCOH by a C−H bond cleavage; after that, the H atom of the OCOH group is abstracted by the OH ligand and finally complex H_2O−Fe^+−O_2C is formed. In the second reaction pathway, complex OFe^+−OCHOH is converted to intermediate HO−Fe^+−OCHO, and then it is converted to the product complex H_2O−Fe^+−O_2C by an H atom migration. Both reaction pathways are likely from the viewpoint of energy, and therefore, the conversion of formic acid to carbon dioxide should easily take place via different routes. The oxidation reactions are energetically accelerated in the final stages. We finally analyzed the energetics for the overall oxidation of methane to carbon dioxide. The overall reaction is exothermic by 117.9 kcal/mol, and there are no high barriers after methanol formation, which can cause the well-known overoxidation problem in methane and alkane oxidation. Formaldehyde and formic acid are not stable in the presence of an excess of oxidants and should be further oxidized to carbon dioxide and carbon monoxide. Our calculations suggest that the

SCHEME 9

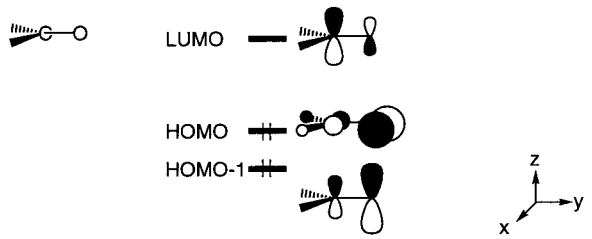

interesting catalytic functions of Fe−ZSM-5 zeolite should arise from a surface iron-oxo species.

Appendix

The resonance explanations in Schemes 3 and 6 are useful, but we look at this from a theoretical point of view. Let us consider perturbation in which the coulomb integral in the carbonyl oxygen α_o will be changed to $\alpha_o + \delta\alpha_o$ by the approach of FeO^+ to the carbonyl oxygen atom.[33] Using the second-order perturbation theory, we can write the deviation of electron densities Δq_s as a function of $\delta\alpha_o$, as shown in the following equation.

$$\Delta q_s = 4\sum_i^{occ}\sum_k^{unocc} \frac{c_s^i c_s^k}{\epsilon_i - \epsilon_k} c_o^i c_o^k \delta\alpha_o \qquad \text{(A1)}$$

Here s is the carbon atom or the oxygen atom of formaldehyde; i and k the orbital index of formaldehyde; c_s^l the orbital coefficient of the s atom in the lth orbital; ϵ_l the lth orbital energy. From eq A1, the mixing between the LUMO and occupied orbitals can determine the electron density change because the next LUMO (LUMO + 1) is high-lying in energy relative to the LUMO. Since the HOMO and the next HOMO (HOMO-1) of formaldehyde lie close in energy, both orbitals can play a role in determining the change of electron densities. The HOMO, the HOMO-1, and the LUMO are shown in Scheme 9. The LUMO is a $p_z\pi^*$ orbital in which the carbon atom has a larger orbital coefficient, whereas the HOMO and the HOMO-1 are $p_x\pi^*$ and $p_z\pi$ orbitals, respectively, in which the oxygen atom has a larger orbital coefficient. Because the p_x and p_z orbitals are orthogonal, the integral of their product is vanished. Thus, the electron density change of the oxygen can be written as eq A2, and that of the carbon atom can be written as eq A3.

$$\Delta q_o = 4\frac{\left(c_o^{HOMO-1} c_o^{LUMO}\right)^2}{\epsilon_{HOMO-1} - \epsilon_{LUMO}}\delta\alpha_o \qquad \text{(A2)}$$

$$\Delta q_c = 4\frac{c_c^{HOMO-1} c_c^{LUMO}}{\epsilon_{HOMO-1} - \epsilon_{LUMO}} c_o^{HOMO-1} c_O^{LUMO}\delta\alpha_o \qquad \text{(A3)}$$

The quantity Δq_o is proportional to the square of the product of c_o^{HOMO-1} and c_o^{LUMO}, whereas Δq_c comes from not only the product of c_o^{HOMO-1} and c_o^{LUMO} but also the product of c_c^{HOMO-1} and c_c^{LUMO}. Because the signs of Δq_o and Δq_c are opposite, the polarizability of the carbonyl group of formaldehyde is increased by the approach of FeO^+. This effect can play an essential role in stabilizing the potential energy surface for the formaldehyde-formic acid conversion by FeO^+.

Acknowledgment. K.Y. is thankful for a Grant-in-Aid for Scientific Research on the Priority Area "Molecular Physical Chemistry" from the Ministry of Education, Science, Sports and Culture of Japan and the Iwatani Naoji Foundation's Research Grant for their support of this work. Computations were partly carried out at the Computer Center of the Institute for Molecular Science.

References and Notes

(1) (a) Shilov, A. E. *The Activation of Saturated Hydrocarbons by Transition Metal Complexes*; Reidel: Dordrecht, The Netherlands, 1984. (b) Shilov, A. E. *Metal Complexes in Biomimetic Chemical Reactions*; CRC: Boca Raton, FL, 1996.

(2) (a) Bergman, R. G. *Science* **1984**, *223*, 902. (b) Arndtsen, B. A.; Bergman, R. G.; Mobley, T. A.; Peterson, T. H. *Acc. Chem. Res*. **1995**, *28*, 154.

(3) Hill, C. L., Ed. *Activation and Functionalization of Alkanes*; Wiley: New York, 1989.

(4) Davies, J. A.; Watson, P. L.; Liebman, J. F.; Greenberg, A. *Selective Hydrocarbon Activation*; VCH: New York, 1990.

(5) (a) Crabtree, R. H. *Chem. Rev*. **1985**, *85*, 245. (b) Crabtree, R. H. *Chem. Rev*. **1995**, *95*, 987.

(6) Gesser, H. D.; Hunter, N. R.; Prakash, C. B. *Chem. Rev*. **1985**, *85*, 237.

(7) Lunsford, J. H. *Angew. Chem., Int. Ed. Engl*. **1995**, *34*, 970.

(8) Schneider, J. J. *Angew. Chem., Int. Ed. Engl*. **1996**, *35*, 1068.

(9) Hall, C.; Perutz, R. N. *Chem. Rev*. **1996**, *96*, 3125.

(10) (a) Taylor, S. H.; Hargreaves, J. S. J.; Hutchings, G. J.; Joyner, R. W. *Methane and Alkane Conversion Chemistry*; Plenum Press: New York. 1995; pp 339−345 (b) Krylov, O. V. *Catal. Today* **1993**, *18*, 209. (c) Yamaguchi, Y.; Teng, Y.; Shimomura, S.; Tabata K.; Suzuki, E. *J. Phys. Chem. A* **1999**, *103* 8272. (d) Yao, S. L.; Takemoto, T.; Ouyang, F.; Nakayama, A.; Suzuki, E.; Mizuno, A. Okumoto, M. *Energy & Fuels* **2000**, *14*, 459.

(11) Anderson, J. R.; Tsai, P. *J. Chem. Soc., Chem. Commun*. **1987**, 1435.

(12) (a) Panov, G. I.; Sobolev, V. I.; Kharitonov, A. S. *J. Mol. Catal*. **1990**, *61*, 85. (b) Sobolev, V. I.; Dubkov, K. A.; Panna, O. V.; Panov, G. I. *Catal. Today* **1995**, *24*, 251. (c) Dubkov, K. A.; Sobolev, V. I.; Talsi, E. P.; Rodkin, M. A.; Watkins, N. H.; Shteinman, A. A.; Panov, G. I. *J. Mol. Catal. A.: Chem*. **1997**, *123*, 155.

(13) Raja, R.; Ratnasamy, P. *Appl. Catal. A. General* **1997**, *158*, L7.

(14) (a) Einhorn, J.; Einhorn C.; Ratajczak, F.; Pierre, J.-L. *J. Org. Chem*. **1996**, *61*, 7452. (b) Vleeming, J. H.; Kuster, B. F. M.; Marin, G. B. *Ind. Eng. Chem. Res*. **1997**, *36*, 3541. (c) Raja, R.; Thomas, J. M. *J. Chem. Soc., Chem. Commun*. **1998**, 1841. (d) Thomas, J. M.; Raja, R.; Sankar, G.; Bell, R. G. *Nature* **1999**, *398*, 227. (e) Sankar, G.; Raja, R.; Thomas, J. M. *Catal. Lett*. **1998**, *55*, 15. (f) Raja, R.; Sankar, G.; Thomas, J. M. *J. Chem. Soc., Chem. Commun*. **1999**, 525. (g) Raja, R.; Sankar, G.; Thomas. J. M. *J. Chem. Soc., Chem. Commun*. **1999**, 829. (h) Raja, R.; Sankar, G.; Thomas. J. M. *J. Am. Chem. Soc*. **1999**, *121*, 11 926.

(15) Yoshizawa, K.; Shiota, Y.; Yumura, T.; Yamabe, T. *J. Phys. Chem. B* **2000**, *104*, 734.

(16) Yoshizawa, K.; Yumura, T.; Shiota, Y.; Yamabe, T. *Bull. Chem. Soc. Jpn*. **2000**, *73*, 29.

(17) A useful review article: Schröder, D.; Schwarz, H. *Angew. Chem., Int. Ed. Engl*. **1995**, *34*, 1973.

(18) (a) Schröder, D.; Schwarz, H. *Angew. Chem., Int. Ed. Engl*. **1990**, *29*, 1433. (b) Schröder, D.; Fiedler, A.; Hrusák, J.; Schwarz, H. *J. Am. Chem. Soc*. **1992**, *114*, 1215. (c) Schröder, D.; Schwarz, H.; Clemmer, D. E.; Chen, Y.-M.; Armentrout, P. B.; Baranov, V. I.; Böhme, D. K. *Int. J. Mass Spectrom. Ion Processes* **1997**, *161*, 175.

(19) (a) Kappes, M. M.; Staley, R. H. *J. Am. Chem. Soc*. **1981**, *103*, 1286. (b) Kappes, M. M.; Staley, R. H. *J. Phys. Chem*. **1981**, *85*, 942.

(20) Schröder, D.; Wesendrup, R.; Schalley, C. A.; Zummack, W.; Schwarz, H. *Helv. Chim. Acta* **1996**, *79*, 123.

(21) (a) Yoshizawa, K.; Shiota, Y.; Yamabe, T. *Chem. Eur. J*. **1997**, *3*, 1160. (b) Yoshizawa, K.; Shiota, Y.; Yamabe, T. *J. Am. Chem. Soc*. **1998**, *120*, 564. (c) Yoshizawa, K.; Shiota, Y.; Yamabe, T. *Organometallics* **1998**, *17*, 2825. (d) Shiota, Y.; Yoshizawa, K. *J. Am. Chem. Soc*. **2000**, *122*, 12 317.

(22) Yoshizawa, K.; Kagawa, Y. *J. Phys. Chem. A* **2000**, *104*, 9347.

(23) (a) Becke, A. D. *Phys. Rev. A* **1988**, *38*, 3098. (b) Becke, A. D. *J. Chem. Phys*. **1993**, *98*, 5648. (c) Stephens, P. J.; Devlin, F. J.; Chabalowski, C. F.; Frisch, M. J. *J. Phys. Chem*. **1994**, *98*, 11 623.

(24) Lee, C.; Yang, W.; Parr, R. G. *Phys. Rev. B* **1988**, *37*, 785.

(25) Frisch, M. J.; Trucks, G. W.; Schlegel, H. B.; Gill, P. M. W.; Johnson, B. G.; Robb, M. A.; Cheeseman, J. R.; Keith, T. A.; Petersson, G. A.; Montgomery, J. A.; Raghavachari, K.; Al-Laham, M. A.; Zakrzewski, V. G.; Ortiz, J. V.; Foresman, J. B.; Cioslowski, J.; Stefanov, B. B.;

Nanayakkara, A.; Challacombe, M.; Peng, C. Y.; Ayala, P. Y.; Chen, W.; Wong, M. W.; Andres, J. L.; Replogle, E. S.; Gomperts, R.; Martin, R. L.; Fox, D. J.; Binkley, J. S.; Defrees, D. J.; Baker, J.; Stewart, J. J. P.; Head-Gordon, M.; Gonzalez, C.; Pople, J. A. *Gaussian 98*, Gaussian Inc.: Pittsburgh, PA, 1998.

(26) Vosko, S. H.; Wilk, L.; Nusair, M. *Can. J. Phys*. **1980**, *58*, 1200.

(27) Wachters, A. J. H. *J. Chem. Phys*. **1970**, *52*, 1033.

(28) Raghavachari, K.; Trucks, G. W. *J. Chem. Phys*. **1989**, *91* 1062.

(29) Krishnan, R.; Binkley, J. S.; Seegar, R.; Pople, J. A. *J. Chem. Phys*. **1980**, *72*, 650.

(30) Loh, S. K.; Fisher, E. R.; Lian, L.; Schultz, R. H.; Armentrout, P. B. *J. Phys. Chem.* **1989**, *93*, 2601.

(31) (a) Shaik, S.; Danovich, D.; Fiedler, A.; Schröder, D.; Schwarz, H. *Helv. Chim Acta* **1995**, *78*, 1393. (b) Schröder, D.; Shaik, S.; Schwarz, H. *Acc. Chem. Res*. **2000**, *33*, 139.

(32) (a) Li, C.; Domen, K.; Maruya, K.; Onishi, T. *J. Catal.* **1990**, *125*, 445. (b) Busca, G. *Catal. Today* **1996**, *27*, 457.

(33) (a) Fukui, K.; Nagata, C.; Yonezawa, T.; Kato, H.; Morokuma, K. *J. Chem. Phys.* **1959**, *31*, 287. (b) Fukui, K.; Morokuma, K.; Yonezawa, T.; Nagata, C. *Bull. Chem. Soc. Jpn.* **1960**, *33*, 963.